Turkish Journal of Engineering & Environmental Sciences

http://journals.tubitak.gov.tr/engineering/

Research Article

Turkish J Eng Env Sci
(2014) 38: 167 – 183

doi:10.3906/muh-1404-6

Simulation approach to study the behavior of a milling machine's structure during end milling operation

Mounir Muhammad Farid KOURA, Muhammad Lotfy ZAMZAM, Amr Ahmed Sayed SHAABAN*
Faculty of Engineering, Ain Shams University, Cairo, Egypt

Received: 16.04.2014 • **Accepted/Published Online:** 15.12.2014 • **Printed:** 30.06.2015

Abstract: This paper presents an integrated simulation system that is employed in order to evaluate the static and dynamic performance of a milling machine. The paper discusses the design consideration of the evaluation system, creates the system based on finite element technique, applies it to a case study, and discusses the results. Obtaining such a reliable model could replace many experimental tests that must otherwise be carried out each time the parameters affecting cutting conditions are changed. Modeling and meshing of various machine elements including the mechanical structure are carried out, contacts between each adjacent elements are defined, load components generated from machining process are modeled, and finally the static and dynamic performance of the entire machine is evaluated. The machine performance is identified in terms of static loop stiffness in both x and y directions, mode shapes, and frequency response function at tool center point.

Key words: Machine tools, static performance, natural frequencies, dynamic behavior, finite element method

1. Introduction

Milling operations are very common in manufacturing. They often represent the last operation, determining the final product quality. The experimental approach to study machining process and machine tool behavior is expensive and time-consuming, especially when a wide range of parameters are included. Hence, virtual prototyping is needed in order to study the effect of various parameters on the machine tool performance. The performance of a machine tool depends on parameters related to the cutting process, such as cutting speed, feed rate, radial and axial depth of cut, and end mill and work piece characteristics, and other parameters related to machine structure, such as structure category, supporting webs, guide-ways stiffness, bolted connections, drive's bearing stiffness, and spindle head position.

The increase in speed of analyses allows for an increased number of concepts to be evaluated and optimized, resulting in a higher quality concept while simultaneously reducing the whole product development time and cost significantly. Among various mathematical models used for simulation, the finite element method (FEM) is proven to be useful and widely used. The FEM is basically defined as dividing a continuous system into small elements. It describes element properties as matrices and assembles them to obtain a system of equations that simulates the behavior of the real system.

Basic ideas of the FEM were studied at the beginning of the 1940s. Courant developed the FEM in 1943 and he used piecewise polynomial interpolation over triangular subregions to model torsion problems [1]. Clough

*Correspondence: amr.ahmed@eng.asu.edu.eg

was the first to use the term "finite element" [2]. Zienkiewicz and Cheung wrote the first book on finite element theory [3]. Other theory books were written by Cook et al. [4], Mohr [5], and Chandrupatla and Belegundu [6]. Researchers usually wrote their own FEM codes for specific processes until the mid-1990s. A foundation and comprehensive information related to the field of virtual machine tool design were presented by Altintas et al. [7]. Integrated dynamic modeling, design optimization, and analysis of a 5-axis ultraprecision micromilling machine were done by Huo and Cheng [8]. In that paper, the finite element model of a high-speed motorized spindle was derived and presented. Moreover, a paper entitled "Modal analysis of machine tool column using FEM" was concerned with providing designers with useful information about static and dynamic behavior of various categories of machine tool columns [9]. In the same context, finite element analysis of bolted joints was developed by Piscan et al. [10]. That paper presented a theoretical model and simulation analysis of bolted joint deformations. Another study that focused on applying virtual prototyping to design a machine tool element was entitled "Virtual design of a machine tool feed drive system" [11]. In order to check the process constraints as well as optimal selection of the cutting conditions for high performance milling, Budak developed analytical models for high-performance milling; milling force, part and tool deflection, form error, and stability models were presented [12]. Finite element analysis of a high-speed motorized spindle based on ANSYS was developed by Liu et al. [13].

In this paper, a system that employs the concept of virtual prototyping is created to provide designers of milling machine tools with useful information and to facilitate improvement of decisions in the early design stage. The desired virtual evaluation system is created using the ANSYS package to evaluate the milling machine tool performance in terms of static loop stiffness, mode shapes, and frequency response frequency (FRF) as illustrated in Figure 1.

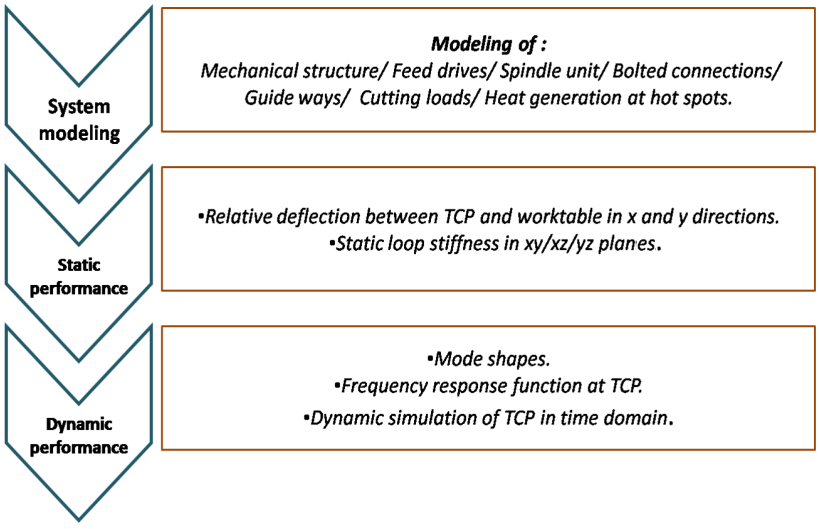

Figure 1. Flow chart of the desired machine tool performance evaluation system.

2. Definition of the evaluation aspects

In this section, the machine tool performance evaluation aspects employed in this paper are discussed. The function of each module, the connection between each, the data entry needed for each, and the results generated are all discussed in detail.

2.1. Static performance of a machine tool

Static analysis calculates the effects of steady loading conditions on the machine while damping effects are neglected. A set of known forces in the x and y directions are applied to the positions of the cutting tool and worktable in order to calculate the relative static deflection between the tool center point (TCP) and worktable. Based on the discussed evaluation aspect, the structural loop stiffness, which characterizes the machine's overall static performance, is calculated. For example, the static loop stiffness (N/μm) in the x direction (YZ plane) includes the saddle, bed, column, screw, slider, and head.

2.2. Dynamic performance of a machine tool

2.2.1. Modal analysis

The natural frequencies and mode shapes are obtained by solving the eigenvalue problem: $[K][X] = \omega^2[M][X]$, where [K] is the stiffness matrix, [X] is the displacement matrix that contains all degrees of freedom and consequently depends on number of nodes, [M] is the mass matrix, and ω is the angular frequency (rad/s). The problem can be satisfied by either [X] = 0, which is a trivial solution, or -[K] – ω^2[M]-= 0, where–is the determent of a given matrix. The eigenvalues ω^2 yield the natural frequencies ω of the system, while the eigenvectors [X] define the mode shapes. The first frequency is usually called the fundamental frequency.

Modal analysis determines the fundamental vibration mode shapes and corresponding frequencies. This study is concerned with the first six natural frequencies and their mode shapes. The first natural frequency is called the fundamental frequency and it indicates the sensitivity of the machine tool to vibration. In this study, modal analysis is established first without putting the effect of the bolts before stress into account. After that, in order to study the effect of the bolts before stress, static analysis is performed prior to modal analysis. While performing modal analysis, all contacts including those between bolted parts are considered linear. No required definition is needed in such a module except the place of fixed support and the FE model of the machine tool. Loads are not allowed to be assigned.

2.2.2. Frequency response function

Harmonic analysis is performed to quantitatively determine the steady-state response of the machine towards sinusoidal loads. Although the cutting forces are varying with time over each tooth interval in a complex manner that is not actually sinusoidal, the cutting forces are repeated for each tooth with a certain frequency that depends on cutting speed. As a result, harmonic analyses are helpful to verify whether or not the design will successfully overcome resonance and harmful effects of forced vibrations.

It should be noted that in conventional machine design, the first natural frequency is expected to be higher than the machine operation frequency. The TCP is almost excited by two harmonic forces in both x and y directions, $F = F_o \sin\omega t$, where ω is the exciting frequency of the cutting forces and F_o is the amplitude of the force, which is assumed to be 1 N.

Two theoretical methods can be applied to generate the FRF; one is the full method and the other is the mode superposition method, which is employed in this paper. The full method gives an exact solution, yet the mode superposition is commonly used because it uses linear iterations to converge the exact values, which takes less computational time. In order to increase the accuracy of the results, a sufficient number of natural frequencies is included.

2.2.3. Dynamic simulation of the TCP in the time domain

During the cutting process, the work piece surface is generated as the cutting teeth intersect with the finished surface. These points are called the surface generation points. As previously mentioned, the cutting load components in the x and y directions can be analytically calculated along the engagement period of one end mill tooth.

Based on the discussed evaluation aspect, the time-varied cutting load obtained from the analytical methods is exported in a tabular form to a transient structure module in ANSYS so as to be subjected to the TCP and worktable. The value of the initial time step is assigned equal to 1/(20 $\times$ the frequency of maximum mode of interest) so as to compromise between computation cost and appropriate resolution. The time-varied deformation in x and y directions generated from the analysis can be used later to evaluate the characteristics of the work pieces surface quality.

3. Modeling of the mechanical structure

3.1. D modeling of mechanical structure

The mechanical structure of a machine tool center can be considered to have the major contribution of its rigidity. It mainly consists of the column, bed, table, saddle, slider, and spindle head. When the cutting process is established on hard materials, the dynamic characteristics of the mechanical structure of a machine tool center become crucial. The CAD model such as that shown in Figure 2 is created using any of the commercial CAD software programs and imported to ANSYS, which is the analysis tool package used in this work. Before creating the FE model of the machine tool structure, small holes, chamfers, fillets, and other tiny details are ignored to simplify the model so that a high-quality mesh can be obtained with minimum computation time.

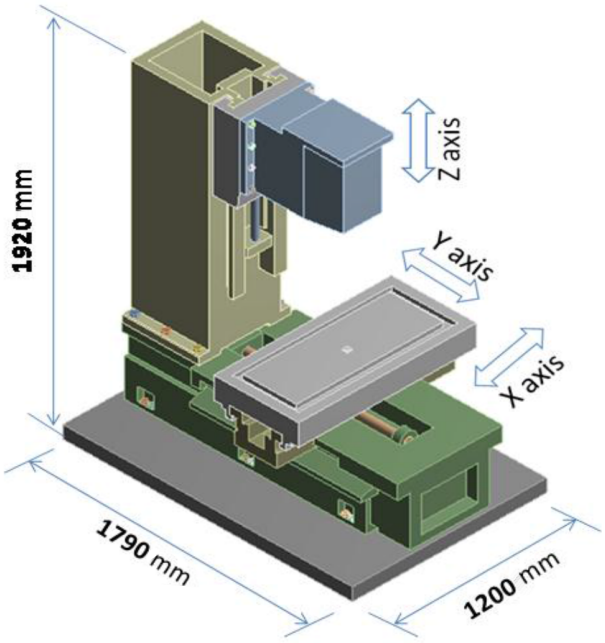

Figure 2. 3D model of a 3-axis open category milling machine tool with main dimensions of 1920 mm $\times$ 1790 mm $\times$ 1200 mm and weight of 4555 kg.

3.2. Contact definition

Contacts are accurately defined to truly describe the actual relation in practice from the aspect of load transfer. For the mechanical structure, the contact between any bolted subsystems such as the column and bed or between any sliding subsystems such as the column and spindle head is defined as frictional with a user-defined coefficient of friction. In the same context, a fixed support is assigned to the lower surface of the machine base as a boundary condition.

The definition of the contact type between any subsystems decides the mathematical relation between the in-contact nodes on both sides. There are three main formulation types: penalty function, Lagrange multiplier, and augmented Lagrange. The last type is preferred in this work.

3.3. FE model of mechanical structure

The FE model of the mechanical substructures is generated from their perspective CAD models using tetrahedron elements. The tetrahedron elements are proven to be more suitable than bricks elements to simulate machine tool structures. Figure 3 shows the FE model of the machine tool mechanical structure. The main characteristic of interest when evaluating a FE model is the mesh size. A fine mesh size leads to converged results, but it increases the degrees of freedom, which increases the computational cost as well. However, local refinements in mesh size can be specified at critical regions such as the TCP and work table using the sphere of influence.

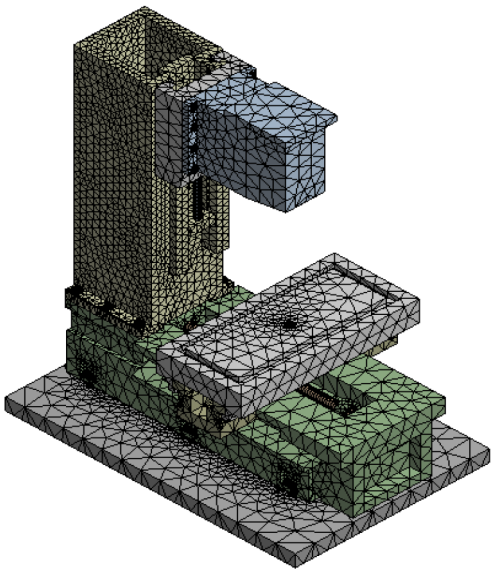

Figure 3. FE model of a 3-axis open category milling machine tool.

To obtain a mesh-independent model with the minimum computation time, constitutive iterations are carried out to properly select mesh characteristics in order to achieve convergence of the results to the exact value within an accepted residual error. The h-method, in which the mesh size is refined until convergence, is employed in this work. This method is preferred for its ease of execution rather than the p-method, in which the degree of polynomial used for the shape function is changed until convergence.

4. Modeling of guide ways

The guide ways are essential elements of a machine tool that support the traverse motions necessary for the cutting process. They have great contribution in affecting the statics and dynamics.

The connection between the sliding parts and the guide ways can be simply represented as a rigid connection at which the contact is defined as bonded and no gap is allowed. However, a rigid connection is not realistic as it considers the guide ways more rigid compared to those in practice. In order to obtain a realistic simulation of the connection between the sliding parts and the guide ways, spring elements are adjusted between each two adjacent surfaces as shown in Figure 4. The spring elements are fitted between the gaps existing between sliding parts and guide ways. Moreover, to ensure that the static stiffness and damping coefficients assigned to the springs truly represent the rigidity of the guide ways, they must be validated against experimental results.

5. Modeling of feed drive units

Screws and drives are essential parts in a machine tool center that are responsible for the traverse motion of both the spindle head and work table. However, they are considered the weakest points from the aspect of dynamic performance, especially when the machine tool is exposed to low-frequency dynamic loads. The feeding system mainly consists of the feed drive, the screw, and the supporting bearings.

The modeling of the feed motor and other accessories is carried out by using lumped masses, while the ball-screw is modeled as a cylindrical rod supported in a simple beam form. The CAD model of the feed drive system is illustrated in Figure 5. The FE modeling of the feed screw is carried out using sweep meshing technique with hexa-dominant elements, which is proven suitable for round parts.

Figure 4. Modeling of machine tool guide ways using spring elements.

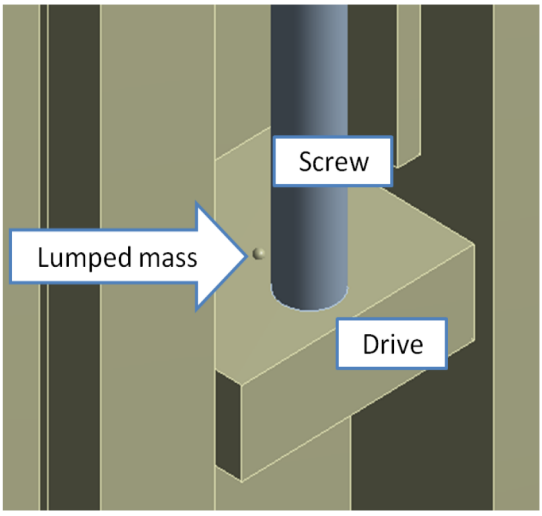

Figure 5. Lumped mass to simulate the machine drives.

As previously discussed in the modeling of guide ways, the contact type between the feed screw, the supporting bearings, and nut are defined as flexible connections at which two springs in the x and y directions (radial) are added between the screw and the nut, and in axial and radial directions between the screw and the supporting bearings. Although the first technique is simpler, the second is more realistic. It is important to

note that the stiffness value of the virtual springs used to simulate the supporting bearings and the nuts must be obtained from experiments.

6. Modeling of machine tool spindle

The spindle assembly mainly consists of the spindle shaft, bearings, sleeves, and driving pulley. The connection between the tool holder and the tool is assumed rigid until this point of investigation. Hence, any deflection that occurs on the spindle nose is assumed to be completely reflected to the TCP.

The whole assembly of the spindle unit is modeled separately and connected rigidly to the spindle housing. The driving pulley, supported bearing, and sleeves are all modeled using lumped masses, while the spindle shaft is modeled as a Timoshenko beam, which is proven to be suitable to its geometry and the stresses exerted on it. Similarly to that in feed drive modeling, the supporting bearings of the spindle shaft are modeled using radial and axial springs of equivalent stiffness. The modeling of the spindle assembly has been previously validated against measurement as detailed in [13].

7. Modeling of bolted connections

The rigidity of the bolted connections used to link several machine substructures contributes in affecting the overall performance of the machine tool. They exist between the bed/column, machine base/bed, and spindle head/slider and are even used in the mounting of machine tool accessories such as motors and drives. In this paper, beam elements are chosen to model the bolted connections. The static stiffness of the beam elements are adjusted equivalent to the bolt's rigidity, and the bolt's preload is defined by applying axial load in each bolt set in an initial time step. Many research studies have been developed in the last decades to model the bolted connections in the machine tool; however, this paper is concerned with the method discussed in [10].

The contact between the bolts' cylindrical bodies and the holes in the corresponding substructures is defined as bonded, while that between the lower surface of the bolts' heads and the surface of the substructure is defined as a frictionless contact. Bolted connections between column/bed and bed/base are shown in Figure 6.

8. Modeling of spindle head position

Any machine tool center must contain moving parts to achieve the necessary motions for the cutting process, known as cutting speed, feed, and depth of cut. The number of moving parts and the type of motions corresponding to them differ according to the machine tool category. The change of the positions of the moving parts leads to a change in the static and dynamic performance of the machine tool, as well.

There are two forms of position dependency. The first is that the position of some parts changes before the cutting process begins, but while the cutting is happening the position remains constant; for example, see the spindle head position in the case of open category milling machine tool shown in Figure 7. In other words, the static and dynamic characteristics of the machine tool will differ according to the depth of the cut. The second form is that the position of some parts changes even during the cutting process, such as, for example, the feed motion of the table or the cross-feed of the saddle.

9. Modeling of the cutting process

To obtain a realistic integrated simulation system, modeling of the cutting process is integrated with the modeling of machine tool mechanical components discussed in the previous subsections. This integration leads to a realistic representation of the overall performance of the machine tool.

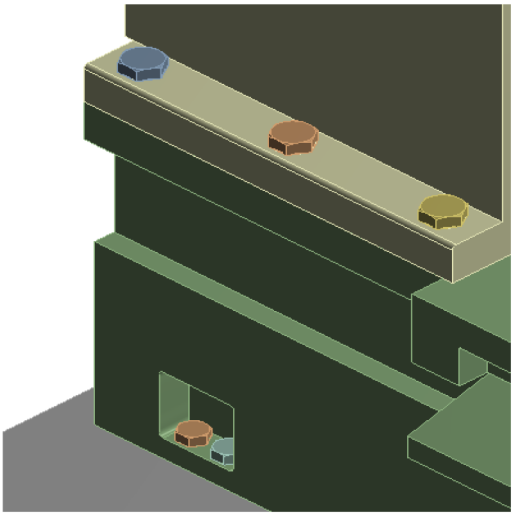

Figure 6. Bolted connections between column/bed and bed/base.

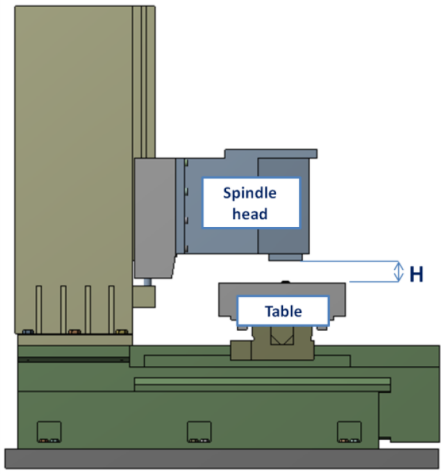

Figure 7. The spindle head position defined by the distance (H) between the TCP and the worktable.

Many works have been carried out on different aspects linked to cutting force prediction. Recently, researchers used the FEM to simulate the cutting process and hence predict the cutting forces and chip morphology. However, simulation of the cutting process using the FEM is not crucial to this paper. An analytical method has been used instead. A cutting force model was developed for conventional end-milling operations [14]. Figure 8 illustrates the cutting mechanics, and the axial and radial depth of cut.

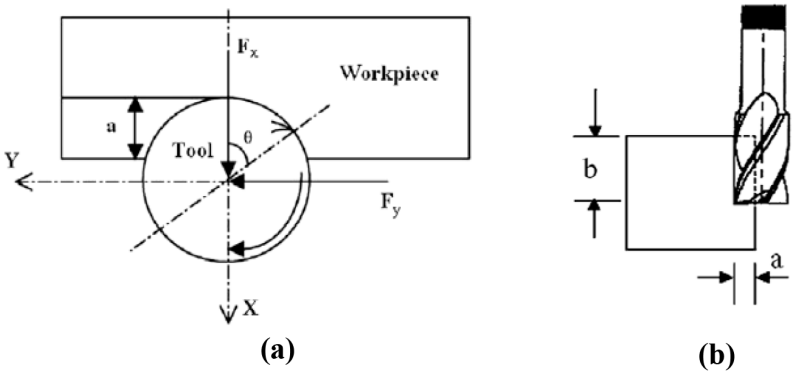

Figure 8. (a) Cutting mechanics, (b) axial and radial depth of cut.

The expressions for the cutting force model were derived as follows.

$$F_x = F_u[(\theta_e - \theta_s) - P_f\left(sin^2\theta_e - sin^2\theta_s\right) - 0.5\left(\sin 2\theta_e - \sin 2\theta_s\right)]$$

$$F_y = -F_u[P_f(\theta_e - \theta_s) - \left(sin^2\theta_e - sin^2\theta_s\right) - 0.5P_f\left(\sin 2\theta_e - \sin 2\theta_s\right)]$$

Meanwhile, $F_u = K_m.r.f_t/tan\beta/2$; $f_t = feedrate/(rpm * no.of\,tooth)$.

F_x is the normal direction cutting force (N), F_y is the feed direction cutting force (N), r is the tool radius (mm), θ_s is the integrating start angle (rad), θ_e is the integrating end angle (rad), β is the helix angle,

f_t is the feed per tooth, the proportional factor P_f was usually selected as 0.3, and K_m is a material factor that can be determined experimentally.

Each cutting edge passes from θ_s to θ_e through three phases.

Phase A: $\theta = [0, \alpha]$

(α:*angle of engagment*)

The cutter is entering the work piece and each rotation d θ increases the length of the edge engaged.

Phase B: $\theta = [\alpha, \emptyset]$, ($\emptyset$:*Contact angle*)

The cutting edge is completely engaged with the work piece, and hence the length of the cutting edge is constant.

Phase C: $\theta = [\emptyset, \emptyset + \alpha]$

The cutting edge begins disengaging the work piece.

Based on the values of the three angles of engagement α, contact $\emptyset$, and tooth angle ψ, one of the following three cases may occur [2].

Case (1): "$\alpha < \varphi$ && $\alpha + \varphi < \psi$"

Θ **[0,** α**]:**

$F_{x1} = F_u\ [\Theta - P_f \sin^2\Theta - 0.5\sin2\ \Theta]$

$F_{y1} = -F_u\ [P_f\Theta - \sin^2\Theta - 0.5P_f \sin2\ \Theta]$

Θ **[**α**,** φ**]:**

$F_{x2} = F_u\ [\alpha - P_f\ (\sin^2\Theta - \sin^2(\Theta - \alpha)) - 0.5(\sin2\Theta - \sin2\ (\Theta - \alpha)]$

$F_{y2} = -F_u\ [P_f\ \ \alpha - (\sin^2\Theta - \sin^2(\Theta - \alpha)) - 0.5\ P_f\ (\sin2\Theta - \sin2\ (\Theta - \alpha)]$

Θ **[**φ**,** $\varphi + \alpha$**]:**

$F_{x3} = F_u\ [(\varphi - \Theta + \alpha) - P_f\ (\sin^2\ \varphi - \sin^2(\Theta - \alpha)) - 0.5(\sin2\varphi - \sin2\ (\Theta - \alpha)]$

$F_{y3} = F_u\ [P_f\ (\varphi - \Theta + \alpha) - (\sin^2\ \varphi - \sin^2(\Theta - \alpha)) - 0.5\ P_f\ (\sin2\varphi - \sin2\ (\Theta - \alpha)]$

Case (2): "$\alpha > \varphi$ && $\alpha + \varphi < \psi$"

Θ **[0,** φ**]:**

$F_{x1} = F_u\ [\Theta - P_f \sin^2\Theta - 0.5\sin2\ \Theta]$

$F_{y1} = -F_u\ [P_f\ \Theta - \sin^2\Theta - 0.5\ P_f\ \sin2\ \Theta]$

Θ **[**φ**,** α**]:**

$F_{x2} = F_u\ [\varphi - P_f\ \sin^2\varphi - 0.5\sin2\varphi]$

$F_{y2} = -F_u\ [P_f\ \ \varphi - \sin^2\varphi - 0.5\ P_f\ \sin2\varphi]$

Θ **[**α**,** $\varphi + \alpha$**]:**

$F_{x3} = F_u\ [(\varphi - \Theta + \alpha) - P_f\ (\sin^2\Theta - \sin^2(\Theta - \alpha)) - 0.5(\sin2\varphi - \sin2(\Theta - \alpha)]$

$F_{y3} = -F_u\ [P_f\ (\varphi - \Theta + \alpha) - (\sin^2\Theta - \sin^2(\Theta - \alpha)) - 0.5\ P_f\ (\sin2\varphi - \sin2(\Theta - \alpha)]$

Case (3): "$\alpha + \varphi > \psi$ "

Case (3) is similar to case (1) except that there is an overlap with value equal to $\alpha + \varphi - \psi$.

10. Construction of the evaluation system

Based on the concepts discussed in the previous sections, the theory based on which the evaluation system is designed can be represented by the chart shown in Figure 9, while the graphic user interface (GUI) of the evaluation system is illustrated in Figure 10. The system's GUI consists of three areas. The system inputs and outputs are defined in Area1, the user-defined design points at which the system runs appear in Area2, and, finally, Area3 shows the charts that represent relationships between specified parameters. All input data and design points that are defined in Area1 and Area2 are automatically transferred to carry out the corresponding analyses without any need to log in to any of the modules; then the generated results are transferred back to be displayed. The system logic and the interconnections between the modules are represented in Figure 11. The data entry of each module and the results generated from each are represented in Table 1. The data are classified as those related to the machine tool, such as 3D model file, spindle head position, characteristics of spring elements, heat generation at hot spots, and bolts pretension, and others related to the cutting process, such as static load at TCP, amplitude and exciting frequency of harmonic loads, and T_c and data sheet of time-varied loads along one tooth interval.

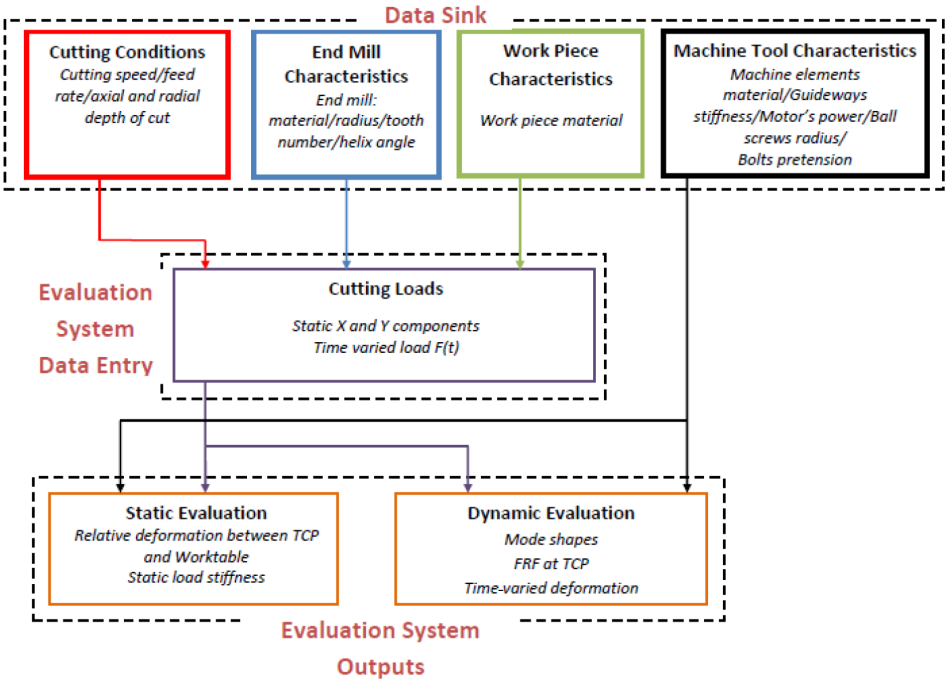

Figure 9. Flow chart of the virtual evaluation system.

11. Application

11.1. Case definition

The virtual evaluation system is applied on a 3-axis milling machine tool of open category. The material of the machine structural components was gray cast iron with modulus of elasticity of 89 GPa, density of 7250 kg/m^3, and Poisson's ratio of 0.25. The cutting process is carried out on a work piece material Inconel718, with set cutting conditions [radial depth of cut (a) = 4 mm, axial depth of cut (b) = 4 mm, feed rate (u) = 100 mm/min, feed per tooth (f_z) = 0.0125 mm/tooth, and cutting speed (s) = 2000 rpm], using an end mill of radius (r) = 10 mm, number of teeth (n) = 4, and helix angle (ß) = pi/6.

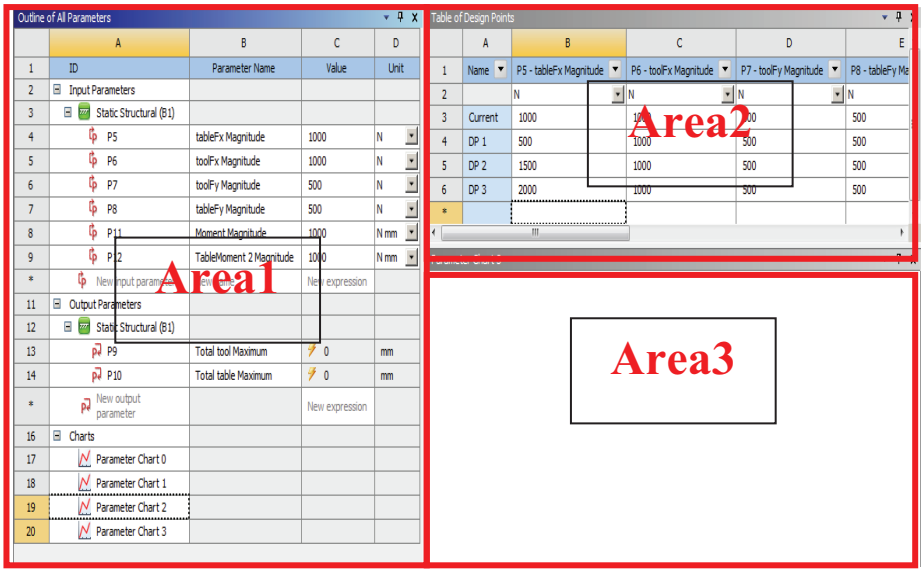

Figure 10. A sample of the input/output panel of the designed evaluation system.

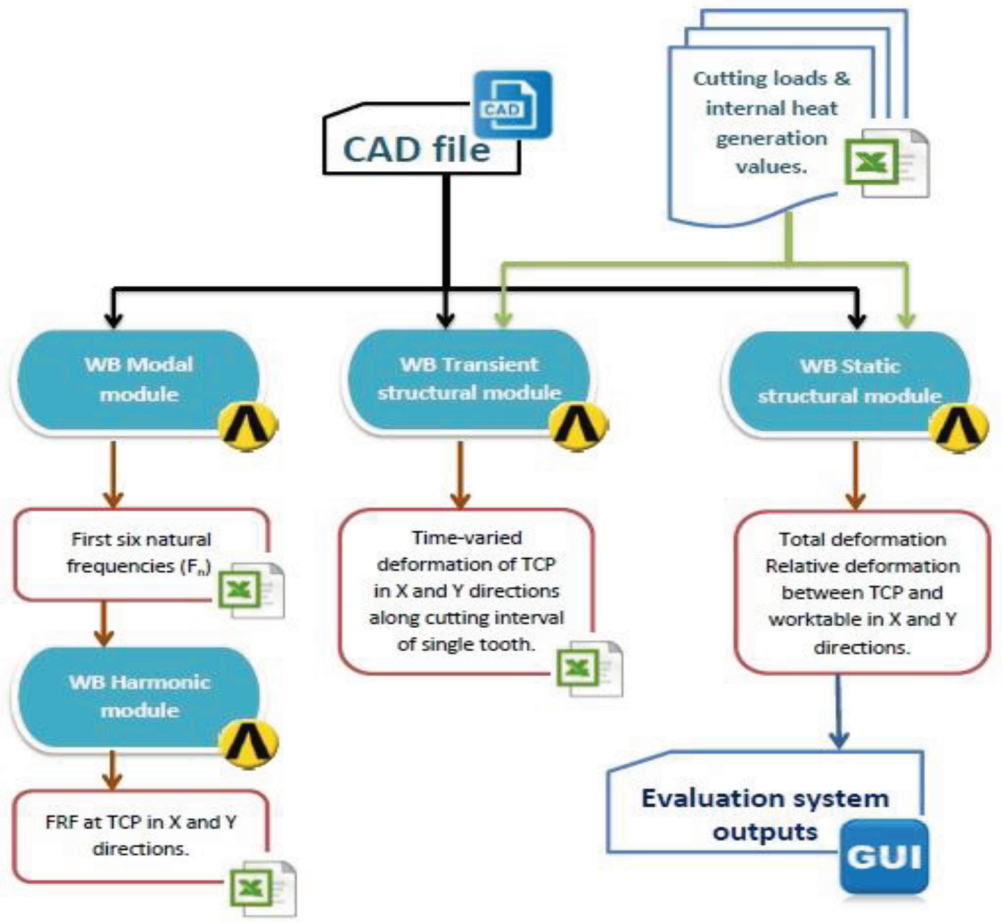

Figure 11. The logic chart of the evaluation system.

Table 1. The evaluation system entries and obtained results from each module.

System entries		Obtained results
Geometry	Spindle head position Cutting load at tcp and worktable	- Directional deformation
Static	in x and y directions Bolt's prestress Static stiffness and damping coefficient of the spring elements	at TCP relatively to worktable in x and y directions
Modal	Only the 3D model	Natural frequencies
Harmonic	Range of exciting frequencies of cutting loads Amplitude of harmonic load at TCP and worktable in x and y directions	FRF at TCP relative to worktable in x and y directions
Time-varied	Tabular data contain time-varied cutting loads within the time period in which one tooth is engaged	Time-varied values of x and y deformations at TCP and worktable

11.2. Preprocessing

11.2.1. Adjusting spindle head position

Before running the system, all data stated in the previous subsection are entered and transferred to each module of the designed system according to its requirements. The spindle head position is adjusted according to the specified depth of cut so that the end mill lower surface is 4 mm below the work piece surface.

11.2.2. Cutting load generation

According to the cutting conditions previously stated in the case definition, the cutting load generated using analytical methods is shown in Figure 12. The graph shows the cutting load values with respect to the end mill angle of rotation along one tooth interval.

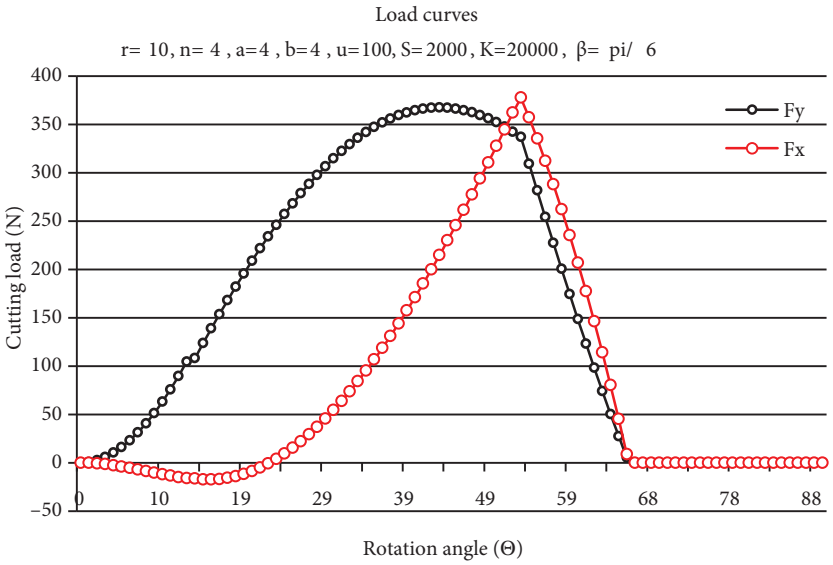

Figure 12. Cutting forces generated along one tooth interval.

11.2.3. Preprocessing of static and dynamic analyses

For the static module, the TCP is subjected to a static load of 1000 N in the x direction and 500 N in the y direction. For the harmonic module, sinusoidal loads of 1 N amplitude with exciting frequency ranges from 30 to 300 HZ frequency are subjected to the TCP. Finally, cutting load values are transferred in a tabulated form to the transient structure module where they are subjected to the TCP through a specified number of time steps so as to obtain the deformation of the TCP during one tooth interval.

11.2.4. Static analysis results

The static analysis performed on the machine tool when subjected to loads previously mentioned shows that the x deformation at the TCP relative to the worktable is equal to 30.7 μm, while the y deformation is equal to 7.1 μm. Generally, in the x direction (YZ plane), the static loop stiffness is found to be equal to 32.5 N/μm, while in the y direction (XZ plane), it is found to be equal to 70.4 N/μm, and therefore the static loop stiffness in the y direction is much better. Figure 13 shows the deformation all over the machine tool structure.

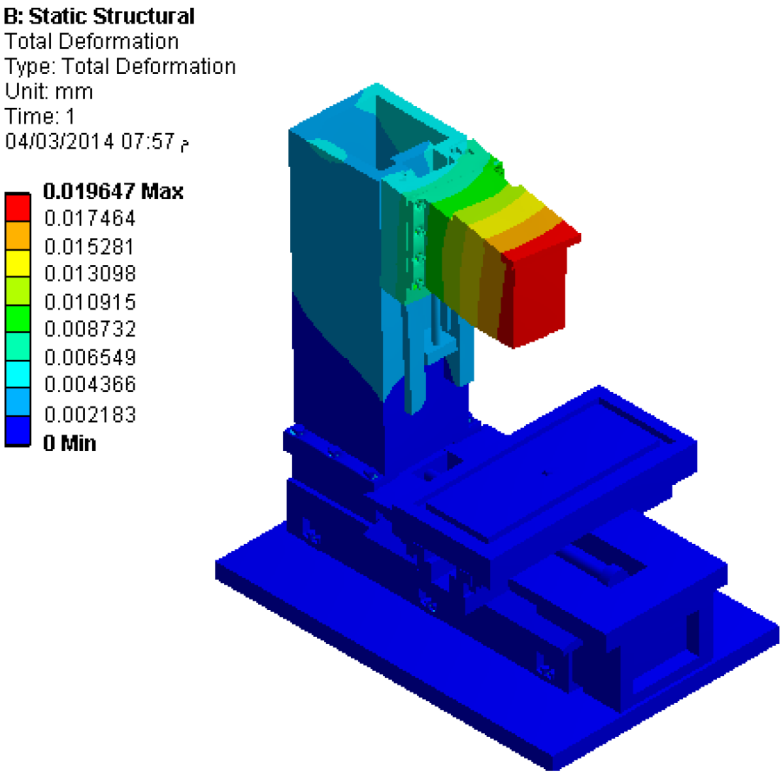

Figure 13. Total deformation all over the machine tool due to static loads Fx = 1000 N and Fy = 500 N at TCP.

11.3. Modal analysis results

Modal analysis has been performed on two cases: first, without including the bolt's prestress effect, and second, when the bolt's prestress effect is included. Figure 14 shows the first six mode shapes of the machine structure in the first case, while Table 2 represents the natural frequencies and the positions of maximum deformation at each mode. From the results obtained in both cases, the first natural frequency is 56 HZ in the first case, while

it is 48 HZ in the second; therefore, the dynamic performance when putting the bolts before stress into account is lower, yet more realistic.

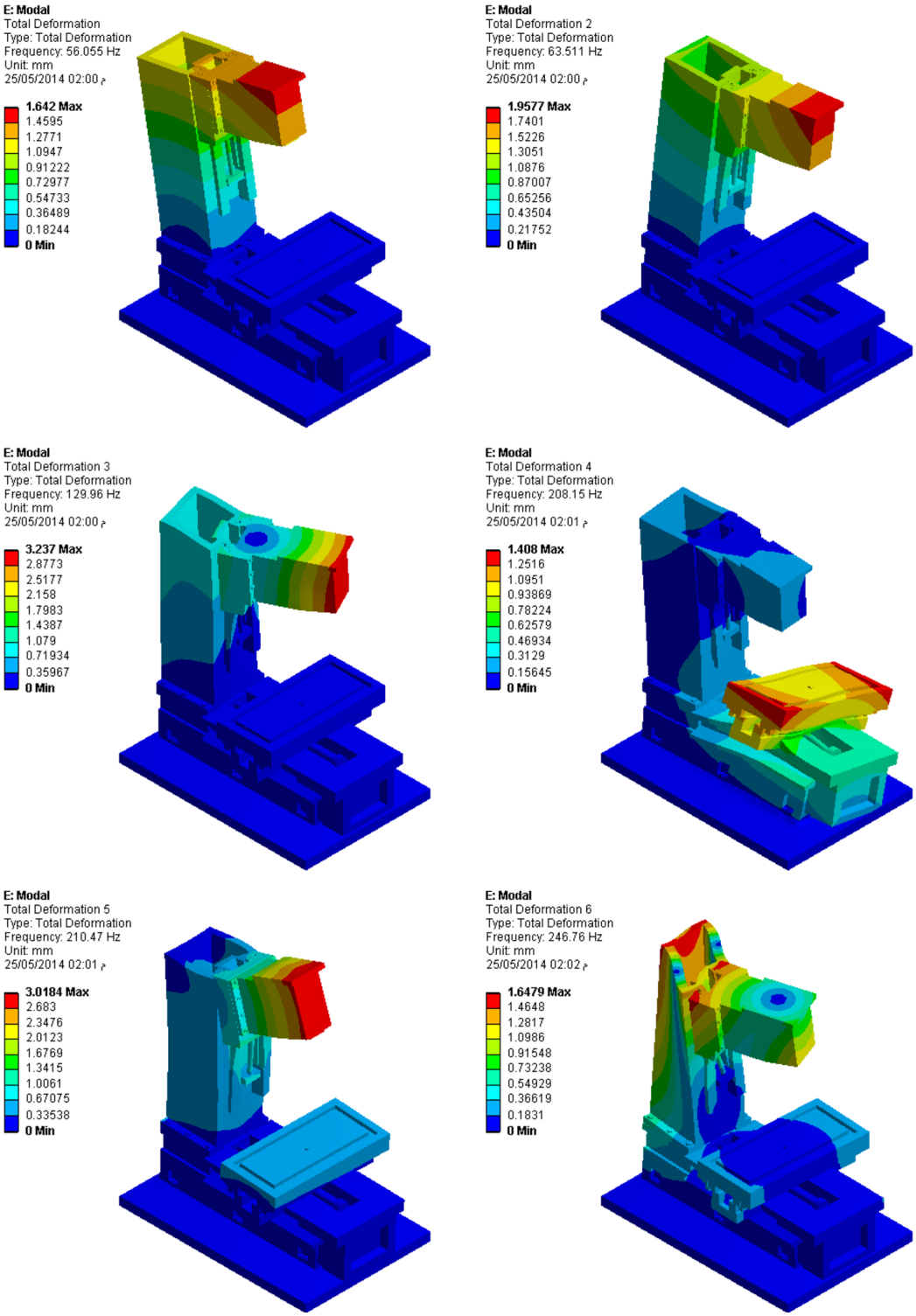

Figure 14. The first 6 mode shapes of the machine tool structure.

Table 2. The first six natural frequencies of the machine tool and the maximum deformation at each mode shape.

	Mode shape	Natural frequencies (HZ)	Position of max deformation
Mode shapes	1	56	Spindle head
	2	63.5	Column
	3	129.9	Spindle head
	4	208.15	Table
	5	210.47	Column screw
	6	246.76	Table

In addition, the first mode shape in both cases is found in the spindle head and the Z slider, and therefore they can be considered the weakest part in the structure. The base and bed show the minimum deformation in almost all mode shapes. The table and saddle begin excitation in the fourth mode shape, and therefore they show better dynamic performance than the Z slider.

11.4. Harmonic analysis results

As evident in Figures 15a and 15b, the maximum dynamic compliance of about 0.12 μm/N in the x direction and 0.05 μm/N in the y direction occurred at 60 HZ, which corresponds to a dynamic stiffness in the XZ and YZ planes of 8 N/μm, and 20 N/μm, respectively. On the other hand, the minimum compliance in the x and y directions occurs at 140 HZ and 180 HZ, respectively. Within the studied range of frequencies, exciting frequencies near 60 HZ should be avoided to prevent harmful resonance effects.

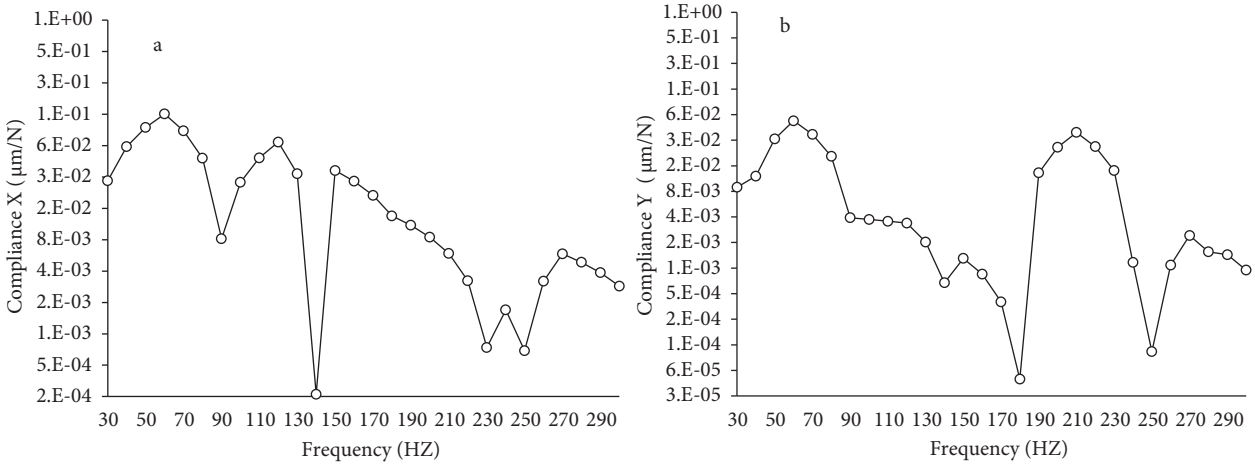

Figure 15. FRF at the TCP in the (a) x direction and (b) y direction.

11.5. TCP deflection during one tooth cycle

The time-varied values of X and Y deformation at both the TCP and worktable are determined as shown in Figures 16a—16d due to the time-varied load subjected to both. The time interval of interest is the engagement period between a single tooth and the work piece, which is equal to 5.51 ms. The determined results can be used later to evaluate the work piece surface quality, and consequently errors and deviations that affect the machine's accuracy can be obtained.

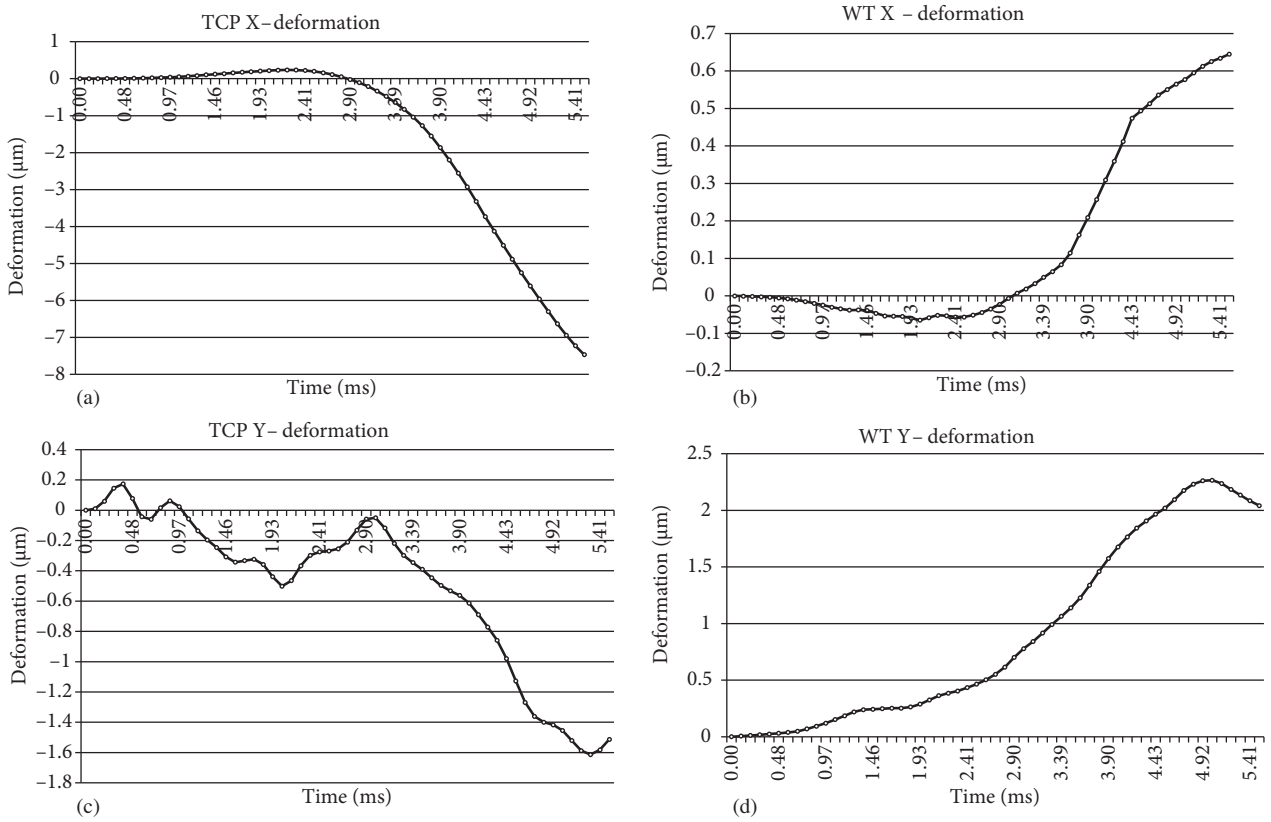

Figure 16. Transient response curve due to time-varied load: (a) x direction at TCP, (b) x direction at worktable, (c) y direction at TCP, and (d) y direction at worktable.

12. Conclusion

An integrated modeling and design approach was developed to create a virtual evaluation system capable of evaluating the static and dynamic performance of milling machine tools during its design stage without the need of prototyping. The modeling of the machine tool mechanical structures and other subsystems together with the modeling of the cutting process were all integrated together to give a comprehensive evaluation of the static and dynamic performance of the entire machine tool. The system was then applied to a case study and the results were represented and discussed in details.

References

[1] Courant R. Variational methods for the solution of problems of equilibrium and vibrations. B Am Math Soc 1943; 48: 1–23.

[2] Clough RW. The finite element method in plane stress analysis. In: Proceedings of the 2nd American Society of Civil Engineers Conference on Electronic Computation, Vol. 23. Pittsburg: PA, USA: ASCE, 1960. pp. 337–345.

[3] Zienkiewicz OC, Cheung YK. The Finite Element Method in Structural and Continuum Mechanics. New York, NY, USA: McGraw-Hill, 1967.

[4] Cook RD, Malkus DS, Plesha ME. Concepts and Applications of Finite Element Analysis. New York, NY, USA: John Wiley & Sons, 1989.

[5] Mohr GA. Finite Element for Solids, Fluids and Optimization. Oxford, UK: Oxford University Press, 1992.

[6] Chandrupatla TR, Belegundu AD. Introduction to Finite Element in Engineering. Upper Saddle River, NJ, USA: Prentice Hall, 2002.

[7] Altintas Y, Brecher C, Weck M, Witt S. Virtual machine tool. Cirp Ann-Manuf Techn 2005; 54: 115–138.

[8] Huo D, Cheng K, Wardle F. Design of a five-axis ultra-precision micro-milling machine—UltraMill. Part 2: Integrated dynamic modelling, design optimisation and analysis. Int J Adv Manuf Tech 2010; 47: 879–890.

[9] Assefa M. Modal analysis of machine tool column using finite element method. International Journal of Mechanical, Industrial Science and Engineering 2013; 7: 51–60.

[10] Piscan I, Predincea N, Nicolae P. Finite element analysis of bolted joint. Proceedings in Manufacturing Systems 2010; 5: 167–172.

[11] Parpală RC. Virtual design of a machine tool feed drive system. UPB Scientific Bulletin Series D 2009; 71: 131–140.

[12] Budak E. Analytical models for high performance milling. Part I: Cutting forces, structural deformations and tolerance integrity. Int J Mach Tool Manu 2006; 46: 1478–1488.

[13] Liu D, Zhang H, Tao Z, Su Y. Finite element analysis of high-speed motorized spindle based on ANSYS. Open Mechanical Engingeering Journal 2011; 5: 1–10.

[14] Saffar RJ, Razfar M, Zarei O, Ghassemieh E. Simulation of three-dimension cutting force and tool deflection in the end milling operation based on finite element method. Simul Model Pract Th 2008; 16: 1677–1688.